Albert, H., et al., 2022, Time scales of open-system processes in a complex and heterogeneous mush-dominated plumbing system: Geology, v. 50, https://doi.org/10.1130/G49934.1

Supplemental Material

Time scales of open-system processes in a complex and heterogeneous mush-dominated plumbing system

Helena Albert, Teresa Trua, José Fonseca, Michael P. Marani, Fabiano Gamberi, Richard Spiess and Andrea Marzoli

Geological setting

The Marsili Volcano (MV) is a large volcanic seamount (ca. 70 km x 20 km) that rises from 3500 m to 500 m below sea level. It has been formed in the last 0.7 Ma in the axial zone of the Marsili Basin (Marani and Trua, 2002; Fig. 1 and Fig. S1), the most recent back-arc basin in the Tyrrhenian Sea opened in relation to retreat of the NW-subducting Ionian slab within the context of African and Eurasian plate convergence (Kastens and Mascle, 1990). Geophysical investigations of the Tyrrhenian Sea (Manu-Marfo et al., 2019 and reference therein) indicate an oceanic nature for the crust underlying the basin, identifying a shallow Moho (10-12 Km). According to ^{14}C geochronological data, submarine explosive eruptions occurred at MV in historical times (Iezzi et al., 2014). The large volume of the MV has prompted geophysical and numerical modeling to detail the potential tsunami hazard due to destabilization of the volcano flanks during or after an eruption, in some cases with significant tsunami impacts along Italian coastlines (Caratori Tontini et al., 2010; Gravina et al., 2019; Gallotti et al., 2021).

The oceanic crust is made of igneous rocks with a hydrous arc-like geochemical affinity (Kastens and Mascle, 1990) also observed in the basaltic to andesitic lava samples dredged from the MV (Fig. 1). In addition, the chemical signatures of the MV lavas provide evidences for the pooling at the crust-mantle transition of a chemically heterogeneous melt, generated by mixing of arc- and Ocean Island Basalt (OIB)-like mantle components (Marani and Trua, 2002; Trua et al., 2011). This petrological scenario is also in line with the wide range of compositions observed in olivine-hosted melt inclusions (Trua et al., 2010) and with the composition of the MV clinopyroxene phenocrysts (Trua et al., 2014).

An extensive sample collection of lavas from the back-arc submarine MV was dredged during the 1998 and 2001 cruises by the ISMAR-CNR Bologna researchers, funded by the MAR98, and TIR2000 CNR

projects. For details on sampling site locations see Trua et al. (2002, 2011) and ISMAR-CNR Bologna data center repository (http://www.ismar.cnr.it/infrastructures/core-repository).

Analytical methods

Major elements in olivine were determined at "Istituto di Geoscienze e Georisorse" of the National Research Council (IGG-CNR) at Padua (Italy) with a CAMECA SX50 Electron Probe MicroAnalyzer (EPMA) equipped with four wavelength dispersive spectrometers (WDS). Analytical conditions were: 15 kV accelerating voltage, 15 nA beam current, peak counting times 15-30 s, and about 1 μm focused electron beam. Standards were natural silicates and metals of known composition. Precision was better than 1% for oxide content higher than 10 wt.%, and better than 3% for oxide content less than 10 wt.%.

The orientation of the crystallographic axes of the modelled olivine crystals were determined by Electron Backscatter Diffraction (EBSD) analysis using a CamScan MX2500 SEM equipped with an LaB6 electron source and a NordlysNano EBSD detector at the Department of Geosciences, University of Padova (Italy). An acceleration voltage of 15 kV, a filament emission current of 450 nA, and a working distance of 25 mm were used.

Thermobarometric conditions used for diffusion modeling

We have quantified the conditions at which olivine crystals from each sample have crystallized by using the MELTS algorithm (Ghiorso and Sack, 1995). We have used the bulk-rock analyses as starting melt composition and have modeled the observed mineralogy (olivine, clinopyroxene, plagioclase and spinel). The specific Fo content of the olivine crystal populations have been considered to better constrain the temperature values used for diffusion modeling. Specific values of temperature, pressure and oxygen fugacity (fO_2) can be found in Table S1. Details about the thermobarometric models can be found in Trua et al. (2018).

Diffusion modeling

We applied the anisotropy correction for each crystal and reported the uncertainty on diffusion times that accounts for analytical (±0.3 Fo mol%) and thermobarometric uncertainty as calculated by DIPRA (Girona and Costa, 2013). In addition, the program calculates the quality of the fit (discrepancy). Our discrepancy values are comprised between 0 and 12%, with 60% of diffusion times obtained from fits with a discrepancy of ≤5% and 99% with <10% (Table S2).

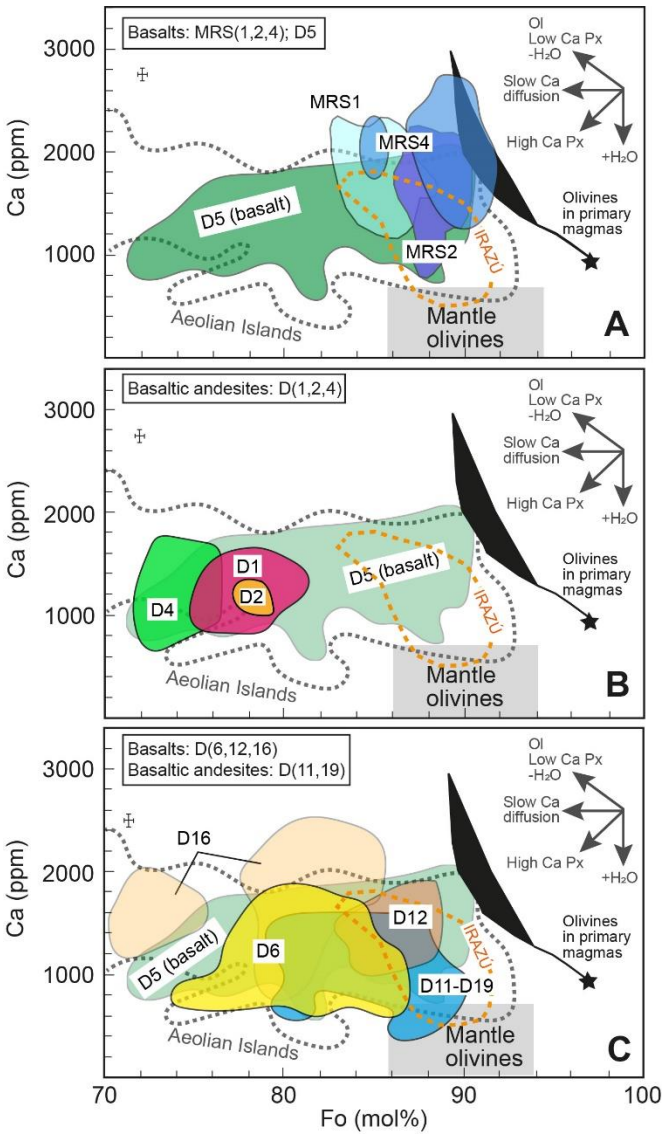

Fig. S1. Forsterite (Fo) versus Ca in olivine crystals from the Marsili Volcano (data from Correia da Fonseca, 2018 and references therein). The black field shows the compositions of olivine crystallizing at the surface from primary melts of anhydrous peridotite, and the arrows indicate the effects of fractionation, slow Ca diffusion and magmatic H_2O dehydration or entry (Gavrilenko et al., 2016). The high magnesian olivine (Fo 89-90), crystallized from primary melts of hydrous peridotite have lower Ca content than the anhydrous sourced ones, as illustrated by the subduction related olivine from the Aeolian Arc (data from Zamboni et al., 2017; grey dotted line field) and the Irazu Volcano (data from Ruprecht & Plank, 2013; orange dotted line field). The grey field for mantle olivine is based on data from Sobolev et al. (2009) and De Hoog et al. (2010).

Table S1. Specific values of temperature (error ±15°C), pressure and fO_2 used for diffusion modeling according to MELTS models (Ghiorso and Sack, 1995).

Sample	Temperature (°C)	Pressure (kbar)	*f*O2 (ΔNNO)
MRS1	1150	0.3	-0.6
MRS4	1170	0.3	0.3
D4	1100	1	-0.7
D5 (high Fo)	1200	2	-0.6
D5 (low Fo)	1170	2	-0.6
D6	1150	1.5	-0.8
D12	1170	1	-0.6
D16	1120	0.5	-0.8

Whole-rock composition included in the Data Repository and in Correia da Fonseca (2018).

Table S2. Time scales calculated by modeling the chemical diffusion of Fe–Mg in olivine crystals.

Olivine	Time (days)	Δ (-)	Δ (+)	Discr. (%)	α	β	γ	P1	P2	P3	B
D4-Ol-1	572	111	145	0	20	105	102	73.4			75.9
D4-Ol-2	826	154	182	0	30	114	73	73.2	74.4		76.2
D4-Ol-3	426	160	134	0	105	25	71	72.9			76.1
D4-Ol-4	976	276	331	6	100	165	80	72.9			74.5
D4-Ol-5	458	87	107	3	20	73	102	73.6	72.7	74	75.8
D5-Ol-3	427	76	99	9	135	47	78	87	82.6		79.7
D5-Ol-4*	601	131	252	0	22	85	65	86.5	89.5	85.6	
D5-Ol-8	1205	202	247	7	82	168	84	77.2	75.9		80
D5-Ol-10*	3361	613	713	3	155	66	92	87.9	82.2		83.2
D5-Ol-11*	548	87	111	7	105	156	72	86.7	87.7		83.1
D5-Ol-13	208	36	42	4	95	6	89	80.5	81.8		75.2
D6-Ol-1	568	156	279	6	15	102	80	86.2	82.4		80.8
D6-Ol-2	57	18	19	7	102	58	145	84.3			81.6
D6-Ol-3	52	17	19	9	102	144	56	83.9			80.8

D6-Ol-4	321	154	130	9	96	159	70	79.9			77.7
D6-Ol-5	18	6	7	0	148	103	63	84			81.1
D12-Ol-1	347	56	80	5	71	157	83	83.5	81.7		84.4
D12-Ol-2	36	11	12	8	78	155	100	86.4			84.5
D12-Ol-4	1069	180	218	8	20	107	115	82.3	87		84.4
D12-Ol-5	313	51	109	9	35	80	122	87.4			83.5
D12-Ol-6	56	21	37	0	153	65	96	86.8			83.5
D16-Ol-1	136	25	31	3	75	145	60	71.9	73.2	70.2	74.8
D16-Ol-4	19	10	17	3	122	34	80	84.3			81.5
D16-Ol-6	301	98	74	4	156	102	57	82.3	81.5		79.7
D16 Ol-8	248	134	64	12	143	48	115	79.4	81.6		
MRS1-Ol-7	4	3	2	0	20	42	10	85.5	85		83.3
MRS1-Ol-8	2977	1155	757	4	170	92	78	85.7			84.2
MRS4-Ol-3	7	5	4	6	135	52	79	88.4	89.2		84.7
MRS4-Ol-4	17	7	11	5	17	92	78	88.3			84.7

P1, P2 and P3 refer to the compositional plateaus observed (numbered from core to rim). B is the boundary composition. We report the angles between the traverses and the three crystallographic axes (α, β, γ) and the discrepancy value (in percentage). The analytical error is ±0.3 for the Fo (mol%). Δ(−) and Δ(+) are the errors on the total time calculated by DIPRA (Girona and Costa, 2013). *Temperature, pressure and fO_2 used for diffusion modeling are indicated in Table S1. Olivine crystals marked with * correspond to "D5 (high Fo)" in Table S1.*

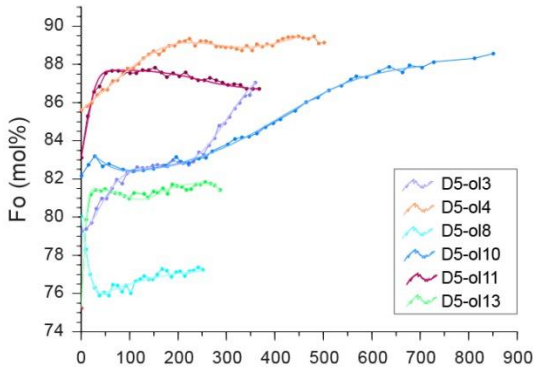
Fo (mol%)
D5-ol3
D5-ol4
D5-ol8
D5-ol10
D5-ol11
D5-ol13

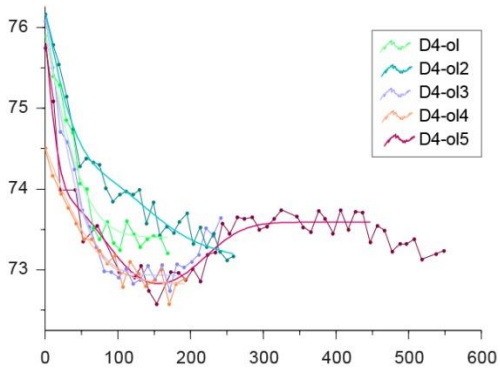
D4-ol
D4-ol2
D4-ol3
D4-ol4
D4-ol5

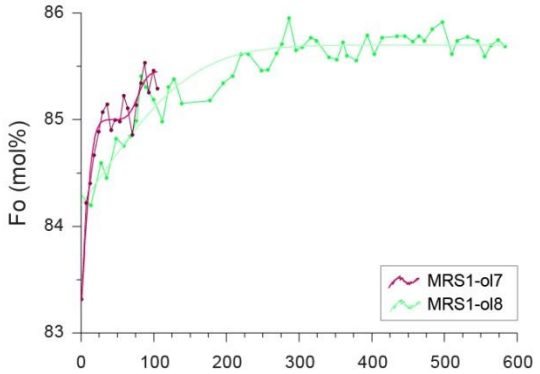
Fo (mol%)
MRS1-ol7
MRS1-ol8

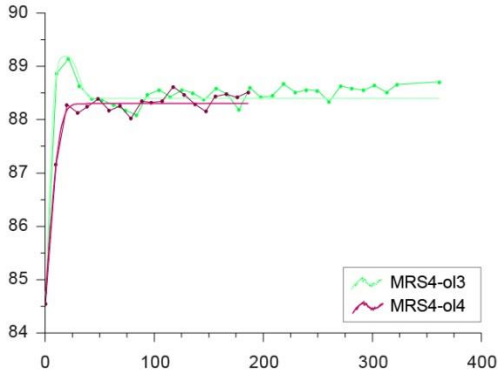
MRS4-ol3
MRS4-ol4

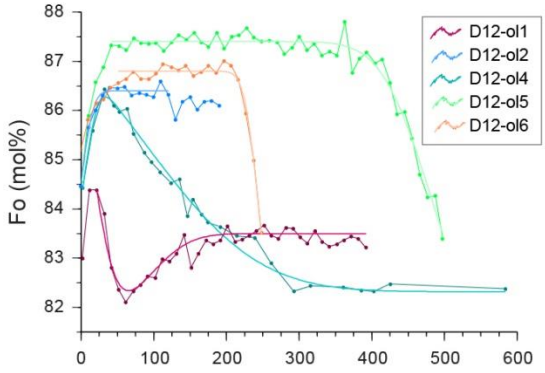
Fo (mol%)
D12-ol1
D12-ol2
D12-ol4
D12-ol5
D12-ol6

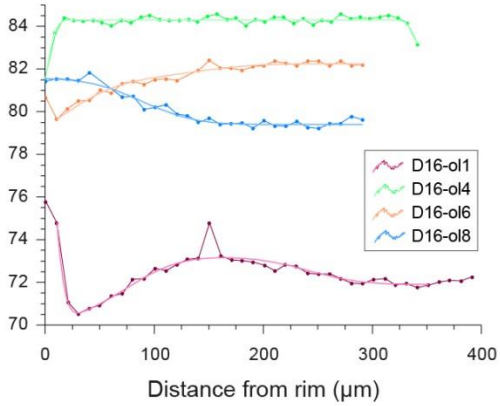
D16-ol1
D16-ol4
D16-ol6
D16-ol8
Distance from rim (µm)

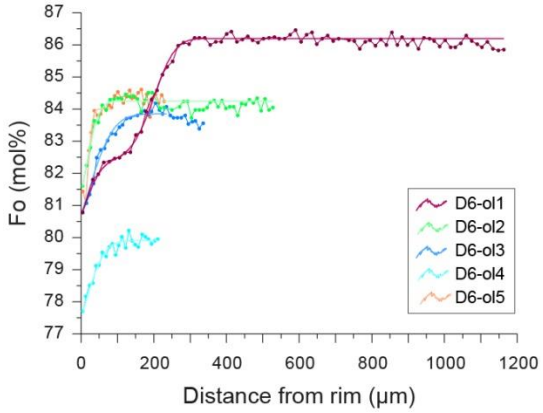
Fo (mol%)
D6-ol1
D6-ol2
D6-ol3
D6-ol4
D6-ol5
Distance from rim (µm)

Fig. S2. Forsterite (Fo) profiles and diffusion modeling in olivine crystals selected from the three main pre-eruptive scenarios (see main text). Olivine profiles from samples D5 and D4 represent the ascent of basic magma fed from a crustal mush layer. Olivine profiles from samples MRS1 and MRS4 are linked to rapid ascent of mantle-derived magma with little crustal interaction. Olivine profiles from samples D12, D16 and D6 evidence mixing between ascending magma and multiple crystal- and melt-rich mush zones.

References cited

Caratori Tontini, F., Cocchi, L., Muccini, F., Carmisciano, C., Marani, M., Bonatti, E., Ligi, M., and Boschi, E., 2010, Potential-field modeling of collapse-prone submarine volcanoes in the southern Tyrrhenian Sea (Italy): Geophysical Research Letters, v. 37, doi:10.1029/2009GL041757.

Correia da Fonseca, J. V. (2018). *Magmatic processes within the plumbing system of the Marsili seamount (Southern Tyrrhenian Sea): constraints from the phenocryst cargo of the sampled lavas* [Thesis Dissertation; Università degli Studi di Parma. Dipartimento di Scienze chimiche, della vita e della sostenibilità ambientale]. https://www.repository.unipr.it/handle/1889/4146.

De Hoog, J.C.M., Gall, L., and Cornell, D.H., 2010, Trace-element geochemistry of mantle olivine and application to mantle petrogenesis and geothermobarometry: Chemical Geology, v. 270, p. 196–215, doi:10.1016/j.chemgeo.2009.11.017.

Gallotti, G., Zaniboni, & F., Pagnoni, & G., Romagnoli, & C., Gamberi, F., Marani, & M., and Tinti, & S., 2021, Tsunamis from prospected mass failure on the Marsili submarine volcano flanks and hints for tsunami hazard evaluation: Bulletin of Volcanology, v. 83, p. 1–15, doi:10.1007/s00445-020-01425-0/Published.

Gavrilenko, M., Herzberg, C., Vidito, C., Carr, M.J., Tenner, T., and Ozerov, A., 2016, A calcium-in-olivine geohygrometer and its application to subduction zone magmatism: Journal of Petrology, v. 57, p. 1811–1832, doi:10.1093/petrology/egw062.

Ghiorso, M.S., and Sack, R.O., 1995, Chemical mass transfer in magmatic processes IV. A revised and internally consistent thermodynamic model for the interpolation and extrapolation of liquid-solid equilibria in magmatic systems at elevated temperatures and pressures: Contributions to Mineralogy and Petrology, v. 119, p. 197–212, doi:10.1007/BF00307281.

Girona, T., and Costa, F., 2013, DIPRA: A user-friendly program to model multi-element diffusion in olivine with applications to timescales of magmatic processes: Geochemistry, Geophysics, Geosystems, v. 14, p. 422–431, doi:10.1029/2012GC004427.

Gravina, T., Mari, N., Farina, L. and Calabria P., 2019, Tsunami risk perception along the Tyrrhenian coasts of Southern Italy: the case of Marsili volcano: Natural Hazards, v. 97, p. 437–454, doi:10.1007/s11069-019-03652-x.

Iezzi, G., Caso, C., Ventura, G., Vallefuoco, M., Cavallo, A., Behrens, H., Mollo, S., Paltrinieri, D., Signanini, P., and Vetere, F., 2014, First documented deep submarine explosive eruptions at the marsili seamount (Tyrrhenian

Sea, Italy): A case of historical volcanism in the mediterranean sea: Gondwana Research, v. 25, p. 764–774, doi:10.1016/j.gr.2013.11.001.

Kastens, K., and Mascle, J., 1990, The geological evolution of the Tyrrhenian Sea: an introduction to the scientific results of ODP Leg 107: Proceedings of the Ocean Drilling Program, Scientific Results, v. 107, p. 26, doi:10.2973/odp.proc.sr.107.187.1990.

Manu-Marfo, D., Aoudia, A., Pachhai, S., and Kherchouche, R., 2019, 3D shear wave velocity model of the crust and uppermost mantle beneath the Tyrrhenian basin and margins: Scientific Reports, v. 9, p. 1–10, doi:10.1038/s41598-019-40510-z.

Marani, M.P., and Trua, T., 2002, Thermal constriction and slab tearing at the origin of a superinflated spreading ridge: Marsili volcano (Tyrrhenian Sea): Journal of Geophysical Research: Solid Earth, v. 107, p. EPM 3-1-EPM 3-15, doi:10.1029/2001jb000285.

Ruprecht, P., and Plank, T., 2013, Feeding andesitic eruptions with a high-speed connection from the mantle.: Nature, v. 500, p. 68–72, doi:10.1038/nature12342.

Sobolev, N. V., Logvinova, A.M., Zedgenizov, D.A., Pokhilenko, N.P., Malygina, E. V., Kuzmin, D. V., and Sobolev, A. V., 2009, Petrogenetic significance of minor elements in olivines from diamonds and peridotite xenoliths from kimberlites of Yakutia: Lithos, v. 112, p. 701–713, doi:10.1016/j.lithos.2009.06.038.

Trua, T., Serri, G., Marani, M., Renzulli, A., and Gamberi, F., 2002, Volcanological and petrological evolution of Marsili Seamount (southern Tyrrhenian Sea): Journal of Volcanology and Geothermal Research, v. 114, p. 441-464, doi:10.l016/S0377-0273(0l)00300-6.

Trua, T., Clocchiatti, R., Schiano, P., Ottolini, L., and Marani, M., 2010, The heterogeneous nature of the Southern Tyrrhenian mantle: Evidence from olivine-hosted melt inclusions from back-arc magmas of the Marsili seamount: Lithos, v. 118, p. 1–16, doi:10.1016/j.lithos.2010.03.008.

Trua, T., Marani, M., and Barca, D., 2014, Lower crustal differentiation processes beneath a back-arc spreading ridge (Marsili seamount, Southern Tyrrhenian Sea): Lithos, v. 190–191, p. 349–362, doi:10.1016/j.lithos.2013.12.014.

Trua, T., Marani, M.P., and Gamberi, F., 2018, Magma plumbing system at a young back-arc spreading center: the Marsili Volcano, Southern Tyrrhenian Sea: Geochemistry, Geophysics, Geosystems, v. 19, p. 43–59, doi:10.1002/2017GC007151.

Trua, T., Marani, M.P., and Gamberi, F., 2011, Magmatic evidence for African mantle propagation into the southern Tyrrhenian backarc region: Special Paper of the Geological Society of America, v. 478, p. 307–331, doi:10.1130/2011.2478(16).

Zamboni, D., Trela, J., Gazel, E., Sobolev, A. v., Cannatelli, C., Lucchi, F., Batanova, V.G., and De Vivo, B., 2017, New insights into the Aeolian Islands and other arc source compositions from high-precision olivine chemistry: Lithos, v. 272–273, p. 185–191, doi:10.1016/j.lithos.2016.12.004.